ChemComm

COMMUNICATION

View Article Online
View Journal | View Issue

Cite this: *Chem. Commun.*, 2018, **54**, 9360

Received 24th May 2018,
Accepted 31st July 2018

DOI: 10.1039/c8cc04139c

rsc.li/chemcomm

Efficient separation of C_2 hydrocarbons in a permanently porous hydrogen-bonded organic framework†

Tae-Ung Yoon,‡[a] Seung Bin Baek, ‡*[b] Dongwook Kim,[c] Eun-Jung Kim,[a] Wang-Geun Lee,[b] Bhupendra Kumar Singh,[b] Myoung Soo Lah,[c] Youn-Sang Bae*[a] and Kwang S. Kim *[b]

A highly robust porous hydrogen-bonded organic framework (HOF) constructed by 4,4′,4″-benzene-1,3,5-triyl-tris(benzoic acid) not only achieves the highest uptakes of ethylene and ethane among the HOF materials, but also exhibits unusual adsorption selectivity of C_2H_6 over other C_2 gases. Besides, it exhibits the second highest acetylene uptake among all the reported HOF materials.

Hydrogen-bonded organic frameworks (HOFs), also referred to as supramolecular organic frameworks (SOFs), are promising porous organic crystalline materials that are self-assembled through multiple hydrogen bonding interactions and other non-covalent interactions like π–π stacking.[1] Over the past few years, HOFs have attracted increasing interests due to their potential applications in several areas including hydrocarbon separation,[2] CO_2 separation,[3] proton conduction,[4] molecular capture[5] and sensing.[6] In addition, compared with other porous materials, they show inherent advantages such as solution processibility, easy purification, and reproducibility by simple recrystallization. However, the multiple non-covalent interactions generally do not guarantee the stability of a porous framework, thus it is difficult to maintain a permanent porosity upon solvent removal. Consequently, we still have witnessed a few permanently porous HOFs to date.

Carboxylic acids play an important role in directing various supramolecular structures and C_3-symmetric planar carboxylic acids are of interest because they can form hexagonal networks with voids through the formation of carboxylic acid dimers.[1,7] In fact, Hisaki and coworkers demonstrated that hexagonal networks prepared with various C_3-symmetric planar carboxylic acids can be used as structural motifs for porous HOFs.[8] Similarly, Zentner and coworkers recently reported a microporous HOF of C_3-symmetric 4,4′,4″-benzene-1,3,5-triyl-tris(benzoic acid) (H_3BTB) *via* a hexagonal (6,3) honeycomb structural motif (Fig. 1a) in ethanol and propanols.[9] The π–π stacking and eight-fold interpenetration of two-dimensional (2D) hexagonal sheets in this HOF-BTB generates one-dimensional (1D) solvent channel in the framework (Fig. 1b). Meanwhile, H_3BTB is also known to form nonporous DMF solvate crystals (H_3BTB–DMF) in *N*,*N*-dimethylformamide (DMF) where the carboxylic acids are masked by DMF molecules, prohibiting the formation of carboxylic acid dimers.[10]

Herein, we report single-component adsorption properties of light hydrocarbons (CH_4, C_2H_2, C_2H_4, and C_2H_6) in a robust microporous hydrogen-bonded organic framework HOF-BTB prepared from the H_3BTB–DMF crystals in methanol. We also report efficient selective separations of C_2/CH_4 binary gas mixtures in HOF-BTB. In our effort to find new self-assembled H_3BTB structures, we found that H_3BTB–DMF crystals readily recrystallize in methanol to

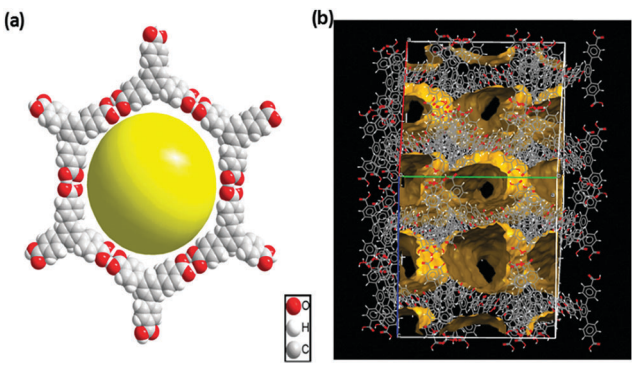

Fig. 1 (a) 2D Hexagonal sheet with a unimodal 3-c hcb (honeycomb) topology in HOF-BTB formed through carboxylic acid dimers. The yellow ball represents a one-dimensional channel with a diameter of *ca.* 25 nm. (b) Solvent-accessible void space of HOF-BTB calculated with the probe radius of 1.4 Å.

[a] *Department of Chemical and Biomolecular Engineering, and Graduate School of Integrated Engineering, Yonsei University, 50 Yonsei-ro, Seodaemun-gu, Seoul 03722, Korea. E-mail: mowbae@yonsei.ac.kr*
[b] *Center for Superfunctional Materials and Department of Chemistry, Ulsan National Institute of Science and Technology (UNIST), 50 UNIST-gil, Ulsan 44919, Korea. E-mail: sepbirth@gmail.com, kimks@unist.ac.kr*
[c] *Department of Chemistry, Ulsan National Institute of Science and Technology (UNIST), 50 UNIST-gil, Ulsan 44919, Korea*

† Electronic supplementary information (ESI) available: Details of experimental procedures, supplementary tables and figures. See DOI: 10.1039/c8cc04139c

‡ These authors contributed equally to this work.

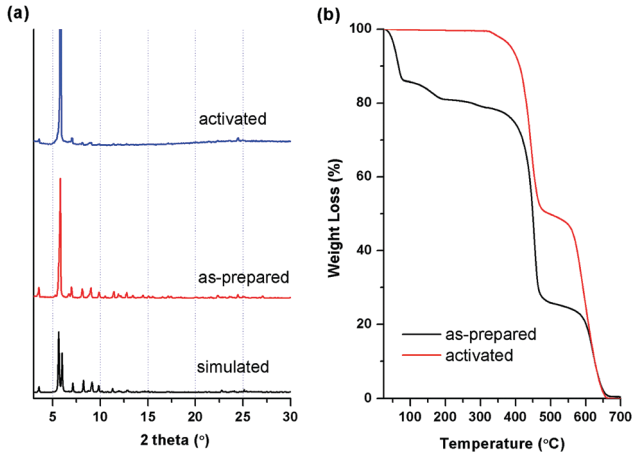

Fig. 2 (a) Powder X-ray diffraction patterns and (b) TGA curves of as-prepared and activated HOF-BTB crystals.

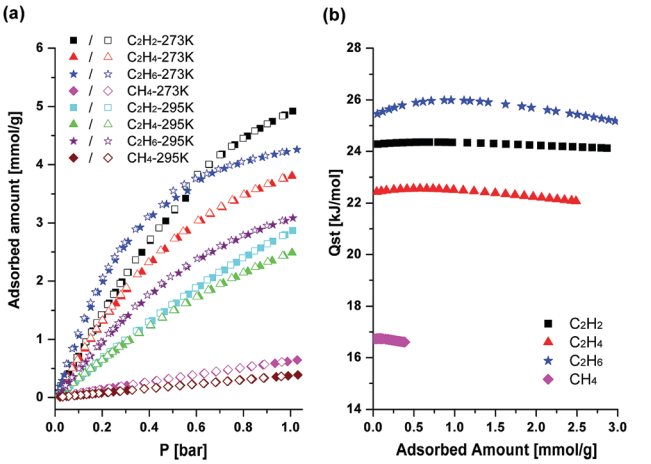

Fig. 3 (a) The adsorption isotherms of HOF-BTB for C_2H_2, C_2H_4, C_2H_6 and CH_4 at 273 K and 295 K, respectively, and (b) loading dependent isosteric heat (Q_{st}) of adsorption. The Q_{st} values were calculated based on adsorption isotherms at 273 K and 295 K by using the Virial method.

produce clear, transparent crystals suitable for single crystal X-ray diffraction. H_3BTB is practically insoluble in methanol so that it is inefficient to attempt direct crystallization of H_3BTB in methanol. Instead, our finding shows that soaking H_3BTB–DMF crystals in methanol at 50 °C facilitates recrystallization of H_3BTB–DMF crystals and the resulting crystals were found to exhibit essentially the same structure as the previously reported HOF-BTB by Zentner.[9] The bulk purity of HOF-BTB crystals is examined by powder X-ray diffraction (PXRD). An observed PXRD pattern of as-prepared HOF-BTB crystals is in good agreement to the simulated PXRD pattern obtained from the reported single crystal structure (Fig. 2a). The crystals of HOF-BTB were treated under high vacuum at 120 °C for 15 hours to generate an activated sample. The PXRD pattern of activated HOF-BTB crystals is identical to that of as-prepared HOF-BTB crystals, which means that the HOF-BTB crystals are very stable even after the removal of solvent molecules. Furthermore, we also found that the immersion of the activated crystals in water for 20 days has no effect on structural stability of the activated HOF-BTB crystals (Fig. S1, ESI†). Thermogravimetric analysis (TGA) curve indicates that HOF-BTB can be stable over 300 °C, resulted from the strong hydrogen bonding interactions as well as the consecutive strong π–π stacking interactions. In addition, the TGA curve of the activated HOF-BTB sample reveals that no residual solvent molecules remain in the activated HOF-BTB (Fig. 2b).

The high stability and the large solvent-accessible void space of HOF-BTB allowed us to investigate its permanent porosity. The N_2 adsorption isotherm of the activated sample obtained at 77 K shows rapid N_2 uptake at relative low pressures ($P/P_0 < 0.1$), which is typical for a Type I isotherm curve and is also typical characteristic for microporous solids (Fig. S2a, ESI†). The total uptake of N_2 at relative pressure $P/P_0 = 1$ is 256 $cm^3\ g^{-1}$. The BET and Langmuir surface areas are estimated to be 955 and 1128 $m^2\ g^{-1}$, respectively. The mean pore diameter and total pore volume are determined to be 16.6 Å and 0.40 $cm^3\ g^{-1}$, respectively. In addition, we calculated micropore size distribution using nonlocal density functional theory (NLDFT) method (Fig. S2b, ESI†). HOF-BTB has a very narrow micropore size distribution of 1.1 to 1.5 nm diameter and a distribution peak at 1.2 nm. The high surface area and total pore volume of HOF-BTB indicates that HOF-BTB possesses a highly porous structure. In order to evaluate the adsorption properties for small hydrocarbons, we performed the adsorption experiments for CH_4, C_2H_2, C_2H_4, and C_2H_6 at 273 K and 295 K, respectively. Fig. 3a shows their adsorption isotherms at both temperatures. All adsorption isotherms are fully reversible in HOF-BTB, indicating pure physisorption processes and easy regeneration of HOF-BTB after gas adsorption. At 273 K, HOF-BTB is the most effective adsorbent for C_2H_2, taking up C_2H_2 up to 110.3 $cm^3\ g^{-1}$ (4.92 mmol g^{-1}) at 1 bar. The uptake capacities of HOF-BTB for C_2H_4 and C_2H_6 are also fairly high at 273 K and 1 bar, with the values of 85.3 $cm^3\ g^{-1}$ (3.80 mmol g^{-1}) and 95.4 $cm^3\ g^{-1}$ (4.25 mmol g^{-1}), respectively. Meanwhile, at 295 K and 1 bar, HOF-BTB shows a higher C_2H_6 uptake (69.2 $cm^3\ g^{-1}$, 3.09 mmol g^{-1}) than C_2H_2 (64.3 $cm^3\ g^{-1}$, 2.87 mmol g^{-1}) and C_2H_4 (55.7 $cm^3\ g^{-1}$, 2.48 mmol g^{-1}) uptakes. Among the C_2 hydrocarbons, C_2H_4 has the lowest adsorption capacities at both temperatures. Interestingly, at 273 K, HOF-BTB adsorbs more of C_2H_6 than the others at lower pressures. As the pressure increases, the adsorption amount of C_2H_2 exceeds the adsorption amount of C_2H_6. At 295 K, on the other hand, the adsorption amount of C_2H_6 exceeds the adsorption amount of C_2H_2 and C_2H_4 in the entire pressure range. This is remarkable because selective adsorption of C_2H_6 over C_2H_2 and C_2H_4 is rarely observed in porous materials including MOFs and zeolites.[11] The higher affinity for C_2H_6, the largest among C_2 hydrocarbons, might suggest that the molecular sizes (C_2H_2, 3.32 × 3.34 × 5.70 Å; C_2H_4, 3.28 × 4.18 × 4.84 Å; C_2H_6, 3.81 × 4.08 × 4.82 Å)[2e] and/or kinetic diameters (C_2H_2, 3.3 Å; C_2H_4, 4.2 Å; C_2H_6, 4.4 Å)[12] of the C_2 hydrocarbons are less important in the adsorption of C_2 hydrocarbons. It might be likely that van der Waals interactions between C_2 hydrocarbons and HOF-BTB are more crucial factor for C_2 hydrocarbons adsorption than the molecular sizes of the gases at lower pressures. The van der Waals interaction is generally stronger as the molecular

Table 1 Comparison of C_2H_2, C_2H_4, and C_2H_6 uptakes in reported HOFs

		C_2H_2 ($cm^3\ g^{-1}$)		C_2H_4 ($cm^3\ g^{-1}$)		C_2H_6 ($cm^3\ g^{-1}$)		Q_{st} ($kJ\ mol^{-1}$)			
HOFs	SA_{BET} ($m^2\ g^{-1}$)	273 K	295 K	273 K	295 K	273 K	295 K	C_2H_2	C_2H_4	C_2H_6	Ref.
SOF-1a	474	61	50	—	—	—	—	36.2	—	—	2*f*
HOF-1a	359	63	57	8.3	3.9	—	—	58.1	31.9	—	2*e*
HOF-3a	165	58	47	—	—	—	—	18	—	—	2*c*
HOF-4a	312	—	—	17.3	11.1	5.1	3.6	—	44	14	2*d*
HOF-5a	1101	182	102	—	—	—	—	27.6	—	—	3*c*
HOF-BTB	955	110.3	64.3	85.3	55.7	95.4	69.2	24.3	22.6	25.4	This work

size increases, so it can be expected that the largest molecule C_2H_6 is the most efficient to interact with HOF-BTB. It should be noted that HOF-BTB achieves the highest C_2H_4 and C_2H_6 uptakes among all the HOF materials reported to date (Table 1). Compared with covalent organic frameworks (COFs), C_2H_6 uptake of HOF-BTB is comparable to most reported COFs. ZnP-CTF-500[13a] and T-COF[13b] outperform the C_2H_6 uptake capacity of HOF-BTB (Table S1, ESI†). Furthermore, C_2H_4 uptake capacity of HOF-BTB surpasses those of the reported COFs such as DBA-3D-COF-1[13c] and MCOF-1.[13d] It also exhibits the second highest C_2H_2 uptake among the HOF materials reported to date. Only HOF-5a exceeds the C_2H_2 uptake amount of HOF-BTB. In contrast to the high C_2 hydrocarbons uptakes, much less amount of CH_4, with the values of 14.5 and 8.7 $cm^3\ g^{-1}$, is adsorbed in HOF-BTB at 273 K and 295 K, respectively. The loading dependent isosteric heats (Q_{st}) of adsorption of C_2 hydrocarbons are larger than that of CH_4, which indicates that the stronger interactions between the C_2 hydrocarbons and the pore surfaces of HOF-BTB than that of CH_4 and HOF-BTB (Fig. 3b). For all the hydrocarbons, the values of Q_{st} remain relatively constant through the whole loading ranges. High affinity for C_2H_6 is also evident in the Q_{st} value. As shown in Fig. 3b, the Q_{st} value of C_2H_6 is higher than those of C_2H_2 and C_2H_4. Compared with other HOF materials, zero-coverage isosteric heats of adsorption for C_2H_2 and C_2H_4 are smaller than those of reported HOFs (Table 1). These lower values of Q_{st} suggest HOF-BTB would be a promising candidate for energy-saving separation of C_2 hydrocarbons/CH_4 mixtures.

To analyse the binary gas mixture separation abilities, the pure single-component isotherms were fitted with the Langmuir–Freundlich isotherm model (Fig. S3–S6, ESI†).[14] Then, ideal adsorbed solution theory (IAST)[15] was used to predict the separation selectivity of binary gas mixtures (50 : 50) at 273 K and 295 K (Tables S2 and S3, ESI†). The IAST predicts that HOF-BTB would allow selective separations of C_2 hydrocarbons over CH_4. At both temperatures, C_2H_6/CH_4 gas mixture shows the highest selectivity values among the C_2 hydrocarbon/CH_4 gas mixtures. The observed C_2H_6/CH_4 selectivity at 295 K (14) is comparable with the IAST-predicted C_2H_6/CH_4 selectivities for N-COF (18), P-COF (12) and T-COF (10) at 298 K.[13b] The IAST also predicts the fairly good separation selectivities for C_2H_2/CH_4 and C_2H_4/CH_4 binary gas mixtures (Fig. 4a and b). Although the IAST can predict the mixture behaviours in terms of adsorption equilibrium, it cannot reflect the mixture behaviours in terms of adsorption kinetics, which cannot be ignored in real adsorption separation processes. Hence, we performed dynamic breakthrough experiments to evaluate the potential of

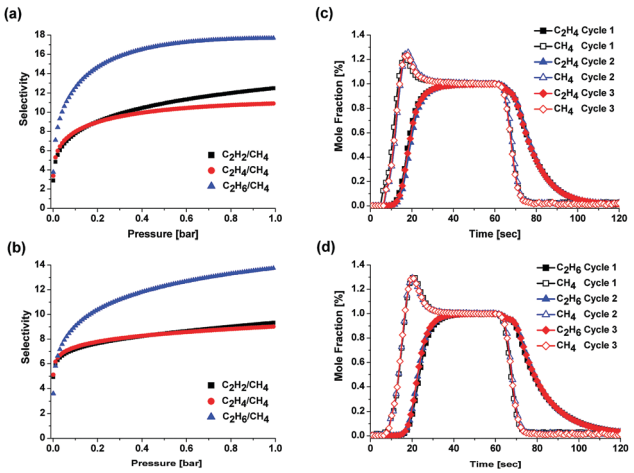

Fig. 4 The IAST-predicted binary gas mixture separation selectivities of HOF-BTB at (a) 273 K and (b) 295 K. The experimental breakthrough curves at three consecutive cycles for a packed-bed filled with HOF-BTB pellets at 298 K and total hydrocarbon pressures of 0.5 bar: (c) equimolar C_2H_4/CH_4 mixture (20 ml min^{-1}); (d) equimolar C_2H_6/CH_4 mixture (20 ml min^{-1}). For each run, 20 ml min^{-1} of He flow was mixed with equimolar hydrocarbon mixture.

HOF-BTB for the adsorptive separation of C_2H_6/CH_4 and C_2H_4/CH_4 mixtures under dynamic flow conditions.[16] Unfortunately, we could not perform the dynamic breakthrough experiment for C_2H_2/CH_4 mixture due to the University's safety regulations. Fig. 4c and d show the experimental breakthrough curves of C_2H_4/CH_4 and C_2H_6/CH_4 mixtures on a column packed with HOF-BTB pellets. In the case of C_2H_6/CH_4 separation, CH_4 elutes first from the column, whereas C_2H_6 is strongly retained. This indicates that under mixture flow condition, HOF-BTB primarily adsorbs C_2H_6 rather than CH_4. Similarly, the breakthrough curves for C_2H_4/CH_4 mixture exhibit selective C_2H_4 adsorption over CH_4. For all cases, breakthrough curves of weaker adsorbate CH_4 show "roll-up" behaviours, which are normally explained as a result of the competitive adsorption between two adsorbate species. Although the weaker adsorbate molecules initially occupy the adsorption sites in the column, some of the adsorbed molecules are replaced by stronger adsorbate molecules.[17] These experimental breakthrough results indicate that HOF-BTB can effectively separate C_2H_4/CH_4 and C_2H_6/CH_4 mixtures under dynamic flow conditions. Easy regeneration of the used adsorbent is an essential consideration for practical operation of an adsorptive separation process. After performing a breakthrough experiment, we regenerated

the column by simply purging it for 10 min under a He flow of 40 ml min^{-1} without heating the column. As displayed in Fig. 4c and d, essentially identical breakthrough curves were produced during the three consecutive cycles for both gas mixtures. This is remarkable because the regenerations were performed under mild conditions. This mild regeneration condition could be attributed to the relatively small Q_{st} values for C_2 hydrocarbons.

In summary, we have reported a highly robust microporous hydrogen-bonded organic framework HOF-BTB, which shows the higher adsorption capacities for C_2 hydrocarbons at 273 K and 295 K. The adsorption amounts of C_2H_4 and C_2H_6 reach the highest values among all the reported HOFs, while C_2H_2 uptake amount reaches the second highest values among all the HOFs. Breakthrough experiments reveal that HOF-BTB can selectively separate C_2H_4 and C_2H_6 from CH_4 under dynamic mixture flow conditions.

This work was supported by NRF (National Honor Scientist Program: 2010-0020414). This work was also supported by the National Research Foundation of Korea under Grant (NRF-2016R1A2B4014256). This work was also supported by ''Next Generation Carbon Upcycling Project'' (Project No. 2017M1A2A2043449) through the National Research Foundation (NRF) funded by the Ministry of Science and ICT, Republic of Korea (2017M1A2A2043449). We acknowledge the Pohang Accelerator Laboratory (PAL) for the use of the synchrotron 2D (SMC) beamline (2017-1st-2D-004 and 2017-2nd-2D-007). Experiments at Pohang Light Source (PLS) were supported in part by Ministry of Science ICT and Future Planning of Korea (MSIP) and Pohang University of Science and Technology (POSTECH).

Conflicts of interest

There are no conflicts to declare.

Notes and references

1 Y.-F. Han, Y.-X. Yuan and H.-B. Wang, *Molecules*, 2017, **22**, 266.
2 (*a*) A. Pulido, L. Chen, T. Kaczorowski, D. Holden, M. A. Little, S. Y. Chong, B. J. Slater, D. P. McMahon, B. Bonillo, C. J. Stackhouse, A. Stephenson, C. M. Kane, R. Clowes, T. Hasell, A. I. Cooper and G. M. Day, *Nature*, 2017, **543**, 657; (*b*) F. Hu, C. Liu, M. Wu, J. Pang, F. Jiang, D. Yuan and M. Hong, *Angew. Chem., Int. Ed.*, 2017, **56**, 2101; (*c*) P. Li, Y. He, Y. Zhao, L. Weng, H. Wang, R. Krishna, H. Wu, W. Zhou, M. O'Keeffe, Y. Han and B. Chen, *Angew. Chem., Int. Ed.*, 2015, **54**, 574; (*d*) P. Li, Y. He, H. D. Arman, R. Krishna, H. Wang, L. Weng and B. Chen, *Chem. Commun.*, 2014, **50**, 13081; (*e*) Y. He, S. Xiang and B. Chen, *J. Am. Chem. Soc.*, 2011, **133**, 14570; (*f*) W. Yang, A. Greenaway, X. Lin, R. Matsuda, A. J. Blake, C. Wilson, W. Lewis, P. Hubberstey, S. Kitagawa, N. R. Champness and M. Schröder, *J. Am. Chem. Soc.*, 2010, **132**, 14457.
3 (*a*) R. S. Patil, D. Banerjee, C. Zhang, P. K. Thallapally and J. L. Atwood, *Angew. Chem., Int. Ed.*, 2016, **55**, 4523; (*b*) S. Nandi, D. Chakraborty and R. Vaidhyanathan, *Chem. Commun.*, 2016, **52**, 7249; (*c*) H. Wang, B. Li, H. Wu, T.-L. Hu, Z. Yao, W. Zhou, S. Xiang and B. Chen, *J. Am. Chem. Soc.*, 2015, **137**, 9963; (*d*) W. Yang, B. Li, H. Wang, O. Alduhaish, K. Alfooty, M. A. Zayed, P. Li, H. D. Arman and B. Chen, *Cryst. Growth Des.*, 2015, **15**, 2000; (*e*) J. Lü, C. Perez-Krap, M. Suyetin, N. H. Alsmail, Y. Yan, S. Yang, W. Lewis, E. Bichoutskaia, C. C. Tang, A. J. Blake, R. Cao and M. Schröder, *J. Am. Chem. Soc.*, 2014, **136**, 12828; (*f*) X.-Z. Luo, X.-J. Jia, J.-H. Deng, J.-L. Zhong, H.-J. Liu, K.-J. Wang and D.-C. Zhong, *J. Am. Chem. Soc.*, 2013, **135**, 11684; (*g*) M. Mastalerz and I. M. Oppel, *Angew. Chem., Int. Ed.*, 2012, **51**, 5252.
4 (*a*) A. Karmakar, R. Illathvalappil, B. Anothumakkool, A. Sen, P. Samanta, A. V. Desai, S. Kurungot and S. K. Ghosh, *Angew. Chem., Int. Ed.*, 2016, **55**, 10667; (*b*) W. Yang, F. Yang, T.-L. Hu, S. C. King, H. Wang, H. Wu, W. Zhou, J.-R. Li, H. D. Arman and B. Chen, *Cryst. Growth Des.*, 2016, **16**, 5831.
5 (*a*) W. Yan, X. Yu, T. Yan, D. Wu, E. Ning, Y. Qi, Y.-F. Han and Q. Li, *Chem. Commun.*, 2017, **53**, 3677; (*b*) T.-H. Chen, I. Popov, W. Kaveevivitchai, Y.-C. Chuang, Y.-S. Chen, O. Daugulis, A. J. Jacobson and O. Š. Miljanić, *Nat. Commun.*, 2014, **5**, 5131.
6 (*a*) H. Wang, H. Wu, J. Kan, G. Chang, Z. Yao, B. Li, W. Zhou, S. Xiang, J. C.-G. Zhao and B. Chen, *J. Mater. Chem. A*, 2017, **5**, 8292; (*b*) Z. Sun, Y. Li, L. Chen, X. Jing and Z. Xie, *Cryst. Growth Des.*, 2015, **15**, 542; (*c*) H. Zhou, Q. Ye, X. Wu, J. Song, C. M. Cho, Y. Zong, B. Z. Tang, T. S. Andy Hor, E. K. Lee Yeow and J. Xu, *J. Mater. Chem. C*, 2015, **3**, 11874.
7 O. Ivasenko and D. F. Perepichka, *Chem. Soc. Rev.*, 2011, **40**, 191.
8 (*a*) I. Hisaki, S. Nakagawa, N. Ikenaka, Y. Imamura, M. Katouda, M. Tashiro, H. Tsuchida, T. Ogoshi, H. Sato, N. Tohnai and M. Miyata, *J. Am. Chem. Soc.*, 2016, **138**, 6671; (*b*) I. Hisaki, S. Nakagawa, N. Tohnai and M. Miyata, *Angew. Chem., Int. Ed.*, 2015, **54**, 3008.
9 C. A. Zentner, H. W. H. Lai, J. T. Greenfield, R. A. Wiscons, M. Zeller, C. F. Campana, O. Talu, S. A. FitzGerald and J. L. C. Rowsell, *Chem. Commun.*, 2015, **51**, 11642.
10 (*a*) S. B. Baek, D. Moon, R. Graf, W. J. Cho, S. W. Park, T.-U. Yoon, S. J. Cho, I.-C. Hwang, Y.-S. Bae, H. W. Spiess, H. C. Lee and K. S. Kim, *Proc. Natl. Acad. Sci. U. S. A.*, 2015, **112**, 14156; (*b*) E. Weber, M. Hecker, E. Koepp, W. Orlia, M. Czugler and I. Csöregh, *J. Chem. Soc., Perkin Trans. 2*, 1988, 1251.
11 (*a*) P.-Q. Liao, W.-X. Zhang, J.-P. Zhang and X.-M. Chen, *Nat. Commun.*, 2015, **6**, 8697; (*b*) Y. Chen, H. Wu, D. Lv, R. Shi, Y. Chen, Q. Xia and Z. Li, *Ind. Eng. Chem. Res.*, 2018, **57**, 4063.
12 J.-R. Li, R. J. Kuppler and H.-C. Zhou, *Chem. Soc. Rev.*, 2009, **38**, 1477–1504.
13 (*a*) H. Ma, H. Ren, S. Meng, F. Sun and G. Zhu, *Sci. Rep.*, 2013, **3**, 2611; (*b*) J. Dong, Y. Wang, G. Liu, Y. Cheng and D. Zhao, *CrystEngComm*, 2017, **19**, 4899; (*c*) L. A. Baldwin, J. W. Crowe, D. A. Pyles and P. L. McGrier, *J. Am. Chem. Soc.*, 2016, **138**, 15134; (*d*) H. Ma, H. Ren, S. Meng, Z. Yan, H. Zhao, F. Sun and G. Zhu, *Chem. Commun.*, 2013, **49**, 9773.
14 J. A. Mason, K. Sumida, Z. R. Herm, R. Krishna and J. R. Long, *Energy Environ. Sci.*, 2011, **4**, 3030.
15 A. L. Myers and J. M. Prausnitz, *AIChE J.*, 1965, **11**, 121.
16 S.-J. Lee, K. C. Kim, T.-U. Yoon, M.-B. Kim and Y.-S. Bae, *Microporous Mesoporous Mater.*, 2016, **236**, 284–291.
17 R. T. Yang, *Adsorbents: Fundamentals and Applications*, John Wiley & Sons, 2003.